Journal of Neuroscience Research

Journal of Neuroscience Research 92:64–73 (2014)

Time Course of Structural and Functional Maturation of Human Olfactory Epithelial Cells In Vitro

Stepahnie Yazinski[1] and George Gomez[2]*

[1]Department of Medicine, Massachusetts General Hospital, Charlestown, Massachusetts
[2]Department of Biology, University of Scranton, Scranton, Pennsylvania

The unique ability of olfactory neurons to regenerate in vitro has allowed their use for the study of olfactory function, regeneration, and neurodegenerative disorders; thus, characterization of their properties is important. This present study attempts to establish the timeline of structural (protein expression) and functional (odorant sensitivity) maturation of human olfactory epithelial cells (hOE) in vitro using biopsy-derived cultured tissue. Cells were grown for 7 days; on each day, cells were tested for odorant sensitivity using calcium imaging techniques and then protein expression of each cell was tested using immunocytochemistry for proteins typically used for characterizing olfactory cells. Previous studies have shown that mature olfactory neurons in vitro attain a unique "phase-bright" morphology and express the olfactory marker protein (OMP). By day 3 in vitro, a variety of cells were odorant-sensitive, including both "phase-bright" and "phase-dark" cells that have previously been considered glial-like cells. The functional maturation of these hOEs appears to take place within 4 days. Interestingly, the emergence of an odorant sensitivity profile of both phase-bright and phase-dark cells preceded the expression of marker protein expression for OMP (which is expressed only by mature neurons in vivo). This structural maturation took 5 days, suggesting that the development of odorant sensitivity is not coincident with the expression of marker molecules that are hallmarks of structural maturation. These results have important implications for the use of hOEs as in vitro models of olfactory and neuronal function.

Key words: neuronal cell culture; neurogenesis; intracellular calcium; odorant sensitivity; olfactory marker protein

The unique ability of the olfactory system to regenerate throughout the adult life span has also made it a useful model for the study of processes related to neurogenesis (Calof et al., 1996, 1998) as well as a system for in vitro studies of neuronal structure and function (Vannelli et al., 1995; Vawter et al., 1996). Characterization of the structural and functional features of human olfactory neurons in vitro and in vivo has shown that these cells possess many of the features typical of neurons in the central nervous system, allowing for their use as a model system for both normal human neurobiology and neural dysfunctions associated with aging and other neurodegenerative disorders (Rawson and Gomez, 2002; Ozedner and Rawson, 2004; Zhang et al., 2004; Matigian et al., 2010; Mackay-Sim, 2012).

In vitro, surviving nonneuronal precursors (basal cells) differentiate along a precise pathway (for review see Calof et al., 1996, 1998; Murdoch and Roskams, 2007), during which mature neurons acquire a distinct morphology and expresses marker proteins typical of mature olfactory neurons. Thus, cultured human olfactory epithelial cells (hOEs) have primarily been identified and characterized by using molecular markers such as the olfactory marker protein (OMP; expressed exclusively by mature olfactory neurons in vivo; Margolis, 1980), neural cell adhesion molecule (NCAM; Murrell et al., 1996), β tubulin III (neuron-specific tubulin [NST]; Roskams et al., 1998), or the G-proteins and enzymes used for odor signaling (G_{olf}, Reed, 1992; adenylyl cyclase III, Bakalyar and Reed, 1990). Additionally, researchers have shown the functional ability of hOE cells in culture to respond to odorant stimulation: cultured cells respond to odorants with changes in $[Ca^{2+}]_i$ that are pharmacologically similar to those seen in olfactory neurons acutely isolated from biopsy samples, indicative of in vitro differentiation and maturation (Gomez et al., 2000; Bormgann-Winter et al., 2009).

However, few studies have established the relationship between structural and functional maturation in vitro in individual hOEs. Thus, for our study, we measured the time course of expression of key molecular markers and correlated the expression of these proteins with the appearance of odorant sensitivity in developing hOEs

Contract grant sponsor: NIH/NIDCD; Contract grant number: RO3DC004954-01A2.

*Correspondence to: Dr. George Gomez, University of Scranton—Biology LSC 395, 204 Monroe Ave., Scranton, PA 18510. E-mail: george.gomez@scranton.edu

Received 15 March 2013; Revised 7 August 2013; Accepted 12 August 2013

Published online 3 October 2013 in Wiley Online Library (wileyonlinelibrary.com). DOI: 10.1002/jnr.23296

in vitro. We established continuous human olfactory cell cultures using previously described techniques (Gomez et al., 2000; Borgmann-Winter et al., 2009). A broad range of molecular markers has been used to characterize structural attributes of olfactory neurons in culture, but we selected molecular markers that gave us the most reliable and consistent results under our experimental conditions: NST, NCAM, growth-associated protein 43 (GAP43; for immature neurons), and OMP (for mature olfactory neurons; for review see Calof et al., 1996, 1998). To study functional maturation, we tested individual hOEs for odorant sensitivity to odorant mixes using $[Ca^{2+}]_i$ imaging techniques previously employed in studies on human ORN function (Restrepo et al., 1993b; Rawson et al., 1997; Gomez et al., 2000); in addition, we tested for the expression of two markers for molecules that participate in cAMP-mediated odor signal transduction, adenylyl cyclase III (ACIII) and G_{olf} (for review see Schild and Restrepo, 1998).

MATERIALS AND METHODS

Cell Culture

Olfactory tissue was obtained from two separate biopsies of the upper middle turbinate and opposing septum from healthy adult volunteers as described previously (Lowry and Pribitkin, 1995; Rawson et al., 1997; Borgmann-Winter et al., 2009). The tissue was then continuously cultured in culture flasks in sterile culture medium (90% Iscove's modified Dulbecco's medium, 10% fetal bovine serum, and 1% penicillin/streptomycin) for two passages, then frozen (90% fetal bovine serum + 10% dimethylsulfoxide at −135°C using standard cryopreservation apparatus) as described previously (Borgmann-Winter et al., 2009). These were a kind gift from Dr. Nancy Rawson at the Monell Chemical Senses Center.

For testing, frozen cells were quick thawed and grown to confluence in culture flasks incubated at 36.5°C with 5% CO_2. Prior to testing, cells were passaged into six-well plates. Cells were used only between their second and fifth passages to maintain optimal cell identity and viability; under these conditions, these cells displayed structural and functional properties that were similar to those of primary cultured cells (Borgmann-Winter et al., 2009).

Immunocytochemistry

Immunocytochemistry was conducted as described previously (Gomez et al., 2000). Briefly, immediately after imaging of a well, cells were fixed with 4% paraformaldehyde for 10 min, rinsed phosphate-buffered saline (PBS), permeabilized, and blocked in 10% normal serum/0.3% Triton X for 30 min. Cells were then incubated in primary antibodies overnight. Primary antibodies used were ACIII (1:2,000; Santa Cruz Biotechnology, Santa Cruz, CA; sc-588), GAP43 (1:500; Sigma, St. Louis, MO; G9264 or SAB4300525), G_{olf} (1:2,500; Santa Cruz Biotechnology; sc-55545), NCAM (1:5,000; Sigma; C9672), NST (1:5,000; Sigma; T8578 or T3952), and goat anti-OMP (1:5,000; a gift from Dr. F. Margolis); previous studies (Gomez et al., 2000; Borgmann-Winter et al., 2009) have shown that these specific antibodies serve as ideal molecular markers for hOEs. For controls, primary antibodies were substituted with nonimmune serum. Antibody visualization was conducted using either fluorescein isothiocyanate (FITC)-conjugated (1:200; Sigma) or peroxidase-conjugated secondary antibodies/ABC peroxidase reagents (Vector, Burlingame, CA), following the manufacturer's instructions. For peroxidase staining, cells were visualized with 3,3′-diaminobenzidine (DAB; Sigma) and viewed and photographed with a Nikon TE2000 microscope. For double-label immunocytochemistry, cells were stained with both FITC- and peroxidase-conjugated secondary antibodies and viewed under transmitted and fluorescence illumination as described previously (Gomez et al., 2000).

For studies correlating structural and functional maturation (Fig. 1), cells tested with imaging techniques (see below) were photographed, fixed, immunostained with DAB visualization, and relocalized on the inverted microscope using previously recorded positions. Staining characteristics of each tested cell were noted. Because cells were grown on six-well plates, we could conduct only single-label immunostaining for these studies.

Odorant Response Testing

For each passage, seven six-well plates were prepared, and hOEs were tested every day for 7 days (day 0 = day of plating). Cells were loaded with the calcium indicator fura-2 by incubation for 1 hr in culture medium supplemented with 1 μM fura-2 and 20 μg/ml pluronic F-127 (Molecular Probes, Eugene OR). The plates were situated on the stage on an inverted fluorescence microscope (Nikon TE2000) fitted with a custom-built, precisely calibrated micrometer. A flow apparatus was then situated on top of the plate; this allowed for a constant superfusion and solution exchange into and out of the well (within 5 sec). Cells were superfused with mammalian Ringer's solution (145 mM NaCl, 5 mM KCl, 1 mM $CaCl_2$, 1 mM $MgCl_2$, 1 mM Na-pyruvate, 20 mM Na-HEPES), high-potassium (high K^+) Ringer's solution (mammalian Ringer's with 135 mM Na^+ substituted equimolarly with K^+), or odorant mixes (mix A: citralva, citronellal, eugenol, geraniol, hedione, menthone, phenylethyl alcohol; mix B: ethyl vanillin, isovaleric acid, lilial, lyral, phenylethylamine, triethylamine; Rawson et al., 1997; Gomez et al., 2000). Each odorant was mixed at a suprathreshold concentration of 100 μM and dissolved in Ringer's. Cells were illuminated with 340- and 360-nm excitation wavelengths via a xenon lamp controlled by a filter wheel (Sutter Instruments, Novato, CA); emitted light was filtered at 510 nm and recorded by an intensified Sony CCD camera. Intracellular calcium concentration ($[Ca^{2+}]_i$) in individual hOEs was monitored throughout the entire cell, because these hOEs do not typically display a polarized or localized response. The average $[Ca^{2+}]_i$ through the entire cell was monitored in real time and quantified analyzed in Merlin imaging software (Perkin Elmer, Norwalk, CT).

Individual odorants mixes A and B and high K^+ were delivered separately for 30–60 sec each in random order. Each stimulus application was followed by a "wash" of Ringer solution for at least 60 sec. Odorant responses for individual hOEs were determined as described previously (Gomez et al., 2000).

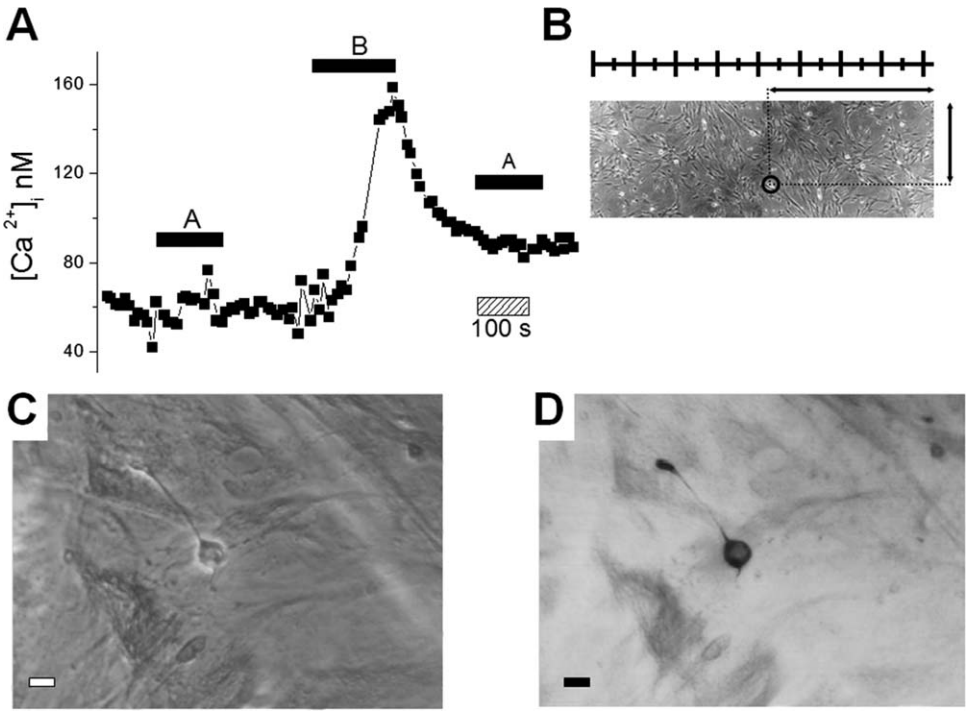

Fig. 1. The method to test the immunocytochemical profile of odorant-sensitive hOEs is outlined. **A:** Odorant responses of individual, visually distinct hOEs were measured using calcium imaging techniques. The solid bar indicates the application of a stimulus solution, the hatched bar indicates a time period (in this case, 100 sec), and the y-axis shows the $[Ca^{2+}]_i$. Upon addition of the stimulus (in this case, odorant mix A or B), the $[Ca^{2+}]_i$ either increased or decreased. Upon removal of the stimulus, the $[Ca^{2+}]_i$ returned to baseline. This particular cell responded to odorant mix B with an increase in $[Ca^{2+}]_i$. **B:** Immediately after the recording, the exact location of the cell in the well was measured using a stage micrometer. **C:** Digital image of the cell was taken for reference (phase-contrast optics, ×40 objective). Immunocytochemistry was then conducted on the entire plate as described in Materials and Methods and stained with DAB. **D:** The hOE was relocalized using the coordinates obtained in B; this cell was $NCAM^+$, as can be seen in the visibly dark staining of the cell compared with the other nonneuronal cells in the same well. Scale bar = 20 μm.

Briefly, if a change in $[Ca^{2+}]_i$ was noted within 5–20 sec following a stimulus application, the $[Ca^{2+}]_i$ began to return to the original resting level within 5–20 sec following stimulus removal, and the magnitude of the $[Ca^{2+}]_i$ change was at least twice that of the normal fluctuation in baseline (no stimulus) $[Ca^{2+}]_i$ values, this was counted as a response (see Fig. 1A for a sample).

Only hOEs that remained viable after delivery of two replicates of the entire stimulus battery (as determined by their fluorescence emission under 360-nm excitation) were counted for data analysis; once cells had completed testing with the stimulus battery, hOEs were photographed under phase-contrast optics, and their exact location in the well was noted using the calibrated microscope stage for subsequent single-label immunocytochemistry (described above). If the cells could not be relocalized accurately following immunostaining, they were not included in the data analysis or cell counts.

Data Analysis

To determine the point at which succeeding days in vitro did not result in an increased in response rate of cells ("steady state"), we used the Welch step-up procedure (Sokal and Rohlf, 1994). To correlate structural and functional maturation, the cells from each treatment day were initially separated into two pools: cells tested with odorants and all the other untested cells in the same well of the six-well plate. For the first pool, the kappa coefficient of agreement was used to determine whether odorant sensitivity is correlated with a particular molecular marker. Briefly, data were tabulated in a 2×2 contingency table according to their dichotomous (+ or −) characteristics. The kappa coefficient compared the probability of co-occurrence of the two events (for example, odorant sensitivity and molecular marker expression) with the probability expected by chance. A value closer to unity implied a tighter correlation between odorant sensitivity and the presence of a particular marker; the null hypothesis was tested with a Yates χ^2 correction. Details of the procedures described above can be found elsewhere (Armitage and Colton, 1998).

RESULTS

Cell Culture

Data for our study were obtained from two separate primary cultures (designated as H523 and H1013) that were frozen at passage 2, thawed, and used from passages 3 to 5. In all of the subsequent data, we found no statistically significant difference in our immunostaining or

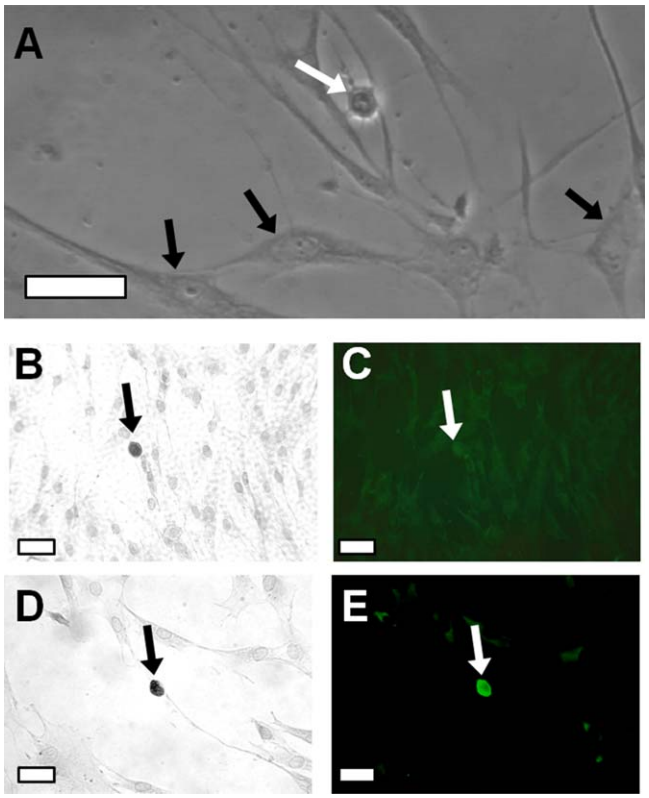

Fig. 2. **A:** Phase-contrast photomicrograph of cells in culture showing two general types of cells. Most of the cells were flattened and triangular and appeared to be phase-dark cells (black arrows). Occasionally, phase-bright cells (white arrow) with distinct neurites were visible. Previous studies (Gomez et al. 2000; Borgman-Winter et al 2009) have focused on the morphological and physiological properties of the phase-bright cells, which express characteristics typical of mature olfactory neurons in vivo: they express OMP (found exclusively in mature olfactory neurons), and they demonstrate odorant-elicited $[Ca^{2+}]_i$ changes that closely approximate the characteristics of acutely isolated human olfactory neurons. For this study, we studied both types of cells. **B–E:** Double-label immunocytochemistry was conducted as described in Materials and Methods; these images show cells stained with ACIII (B,D) and OMP (C,E). B and C show the same cell (arrows) that is $ACIII^+$ and OMP^-; D and E show another cell (arrows) immunopositive for both marker molecules. The background staining was slightly intensified to show the other cells in the culture. Scale bar = 40 μm. [Color figure can be viewed in the online issue, which is available at wileyonlinelibrary.com.]

calcium imaging results between different passages of the same cell line or between data from the two different cell lines ($P > 0.05$, ANOVA), so results for the different passages and the different cell lines were pooled.

These heterogeneous cultures consisted of a variety of cell types that exhibited morphology similar to that shown in previous studies (Wolozin et al., 1992; Gomez et al., 2000; Borgmann-Winter et al., 2009). The majority of the hOEs were flat, triangular, and appeared dark under phase-contrast illumination ("phase-dark" or PD; Fig. 2A, black arrows), which are characteristic of the glial cells that support neuronal cell growth (Ensoli et al., 1998; Higginson and Barnett, 2011). At 0–1 day postpassage, the culture consisted entirely of PD cells, suggesting that mature olfactory neurons did not survive the passage. Phase-bright (PB), circular, rounded cells with distinct processes emerged after 1 day in culture and were present in smaller numbers (Fig. 2A, white arrows). These cells were identified in previous studies as olfactory neurons (Morrison and Costanzo, 1992; Gomez et al., 2000; Borgmann-Winter et al., 2009) by the presence of OMP and by their ability to respond to odorants with mechanisms similar to those seen in acutely isolated human olfactory neurons. The number of PB cells increased as time progressed until about the fifth day in culture, when the ratio of PD to PB cells remained the same.

TABLE I. Double-Label Immunocytochemistry of PB hOEs: hOEs After Day 5 Were Visually Identified and Then Their Antibody Staining Pattern for Two Antibodies Was Noted (Numbers of Cells Tested per Antibody Combination Are Indicated in Parentheses)*

First/second marker (N)	First only	Second only	Both
G_{olf}/ACIII† (46)	0	13	87
G_{olf}/GAP43 (59)	66	12	22
NST/ACIII† (86)	7	14	79
NST/GAP43 (60)	53	0	47
NST/G_{olf} (50)	34	8	58
NST/NCAM† (78)	0	5	95
OMP/ACIII† (50)	0	16	84
OMP/GAP43 (41)	39	61	0
OMP/G_{olf}† (50)	0	18	82

*For column 1, the first marker was detected with DAB and the second with FITC. Numbers in columns 2–4 are expressed as a percentage of total number hOEs viewed for each antibody pair.
†Statistically significant correlation between the two markers (kappa coefficient, $P < 0.05$) as discussed in Materials and Methods.

Our goal was to study the maturation of olfactory neurons in vitro, so we focused our studies on characterizing the PB hOEs using a subset of marker molecules that have been used in previous studies using human olfactory tissue. We fixed and double labeled cells from the two different cell lines at 5 days in vitro; results are shown in Table I. For each marker pair, we counted all the cells from three 22- × 22-mm coverslips from each of the cell lines. We did not notice a significant difference in the results between the two cell lines, so the data from the two cell lines were pooled. Representative immunostaining results are shown in Figure 2. Typically, immunostaining in these cells did not show any subcellular localization: protein was typically distributed throughout the cell. Our double-labeling studies did not show a marked difference in sensitivity between DAB and FITC visualization methods. Figure 2B,C shows the same cell that was $ACIII^+$ and OMP^-, and Figure 2D,E shows a different cell that was $ACIII^+$ and OMP^+. As expected, there was a tight correlation between markers such as NST and NCAM, and nearly all PB hOEs expressed both these molecules (Table I). G_{olf} and ACIII, which both participate in odorant signaling, were also present in most, but not all, PB hOEs. Interestingly, there was no overlap between OMP and GAP43, supporting the notion that

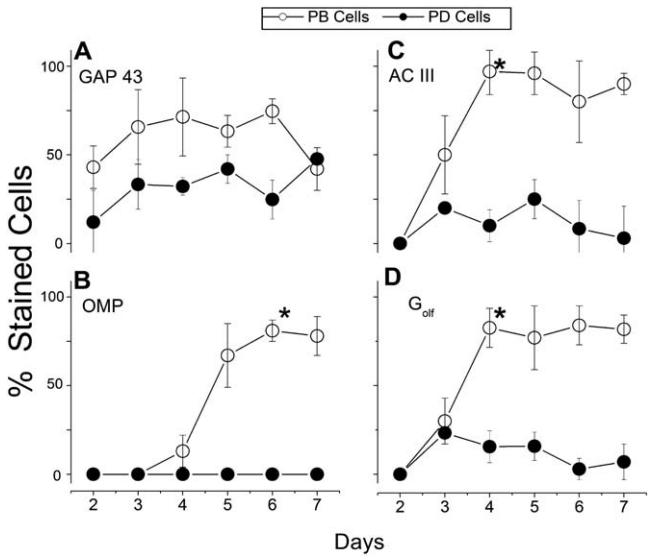

Fig. 3. Marker molecule expression pattern of hOEs changed over time in vitro. hOEs were passaged onto glass coverslips at day 1 and grown in a large culture dish. Every day from day 2 to day 7, individual coverslips were separated and immunostained for the structural (GAP43 and OMP, left) and functional (ACIII and G_{olf}, right) marker proteins; staining was visualized with DAB. The data are from eight individual repetitions. Cells were visually identified under phase contrast as phase-bright (PB) cells, and we also looked at the phase-dark (PD) cells that surrounded them as internal controls; their immunostaining profile was then determined under transmitted light. Day 1 was not tested because at this time very few PB cells are present. The proportion of stained cells was determined for all cells viewed on each coverslip; because the PD cells outnumbered the PB cells, the percentages of stained PD and PB cells were not directly comparable. Note that none of the PD cells stained for OMP. Asterisks indicate the point at which responses attained a "steady state" (Welch step-up procedure; for details see Materials and Methods).

GAP43 is expressed exclusively by immature neurons. There were also some cells that expressed G_{olf} or ACIII that were not OMP positive.

Time Course of Structural Maturation

Given the double-labeling results, we quantified the structural maturation time course of the PB hOEs using a subset of four marker molecules, OMP, GAP43, ACIII, and G_{olf}. Previous studies on olfactory neuron differentiation suggest that GAP43 is expressed by differentiating neurons (Schwob, 2002), whereas OMP is expressed upon maturation (Margolis, 1980; Morrison and Costanzo, 1992). ACIII and G_{olf} are proteins used in odor signal transduction. Because we used a heterogeneous culture, the PD cells that accompanied the PB hOEs served as an internal control.

Figure 3 shows the summary data for eight iterations of the experiment. A large proportion of PB hOEs ranging from day 3 to day 7 was stained for GAP43, and these cells were distinctly identified as positive or negative, suggesting that some PB cells were still early in the differentiation process while others were in a more advanced stage of development. The number of either PB or PD cells that were stained positively for GAP43 did not follow any trend as the cell culture matured: at no point did staining percentages attain a steady state (Welsch step-up procedure, $P > 0.05$). As expected, OMP was seen only in PB cells, consistent with findings from previous studies (Wolozin et al., 1992; Murrell et al., 1996; Gomez et al., 2000). Interestingly, although ACIII and G_{olf} expression in PB hOEs increased by day 4, and then attained a steady state, a small proportion of PD cells also expressed these two marker molecules, suggesting that these cells were possibly differentiating olfactory neurons.

Time Course of Functional Maturation

Odorant-elicited $[Ca^{2+}]_i$ changes. Previous studies have shown that hOEs responded to odorant stimulation using mechanisms that were similar to those found in acutely isolated in human ORNs (Gomez et al., 2000); therefore, we focused our attention on these PB hOEs (n = 704) and tested their odorant sensitivity using odorant-elicited $[Ca^{2+}]_i$ changes. The data shown are summed from 14 individual runs. Both PB and PD cells loaded with fura-2; thus, the PD cells served as an internal control. To allow ratiometric imaging of both cell types, exposure time for image acquisition was lengthened to 500 msec (when recording from PB hOEs only, usually 100–200 msec exposure times would suffice). This expectedly reduced the sensitivity of the recordings of the PB cells but did not influence the results because the presence and direction of responses were still clearly recognizable. In addition, we ensured that the emitted light intensity was not near the end of the dynamic range of our camera. Our pilot studies showed that increasing the exposure time from 200 to 500 msec did not affect the ratiometric data that we acquired from the PB hOEs.

As can be seen in Figure 4A, the proportion of odorant-sensitive PB hOEs increased steadily from day 3 to day 5 and maintained a response rate of 34–38% through day 7; this proportion was similar to that seen in previous studies on hOEs (Gomez et al., 2000). Interestingly, approximately 25% of the PD cells also responded to odors; this proportion remained consistent from day 3 to day 7.

A breakdown of the details of Figure 4A is provided in Figure 4B. In the human ORNs and hOEs, responses to odorants could be either increases or decreases in $[Ca^{2+}]_i$, with increases in $[Ca^{2+}]_i$ typically occurring twice as frequently as decreases (for review see Rawson and Gomez, 2002). In previous studies on hOEs (Gomez et al., 2000), these response rates were typically measured at day 5; our data for response rates at day 5 were consistent with these previously published results. It is interesting to note that, at early stages of the culture (days 3 and 4), increases and decreases in $[Ca^{2+}]_i$ are seen with equal frequency. At day 5, however, there is a significant difference (χ^2, $P < 0.05$) between odorant-elicited $[Ca^{2+}]_i$ increases and decreases.

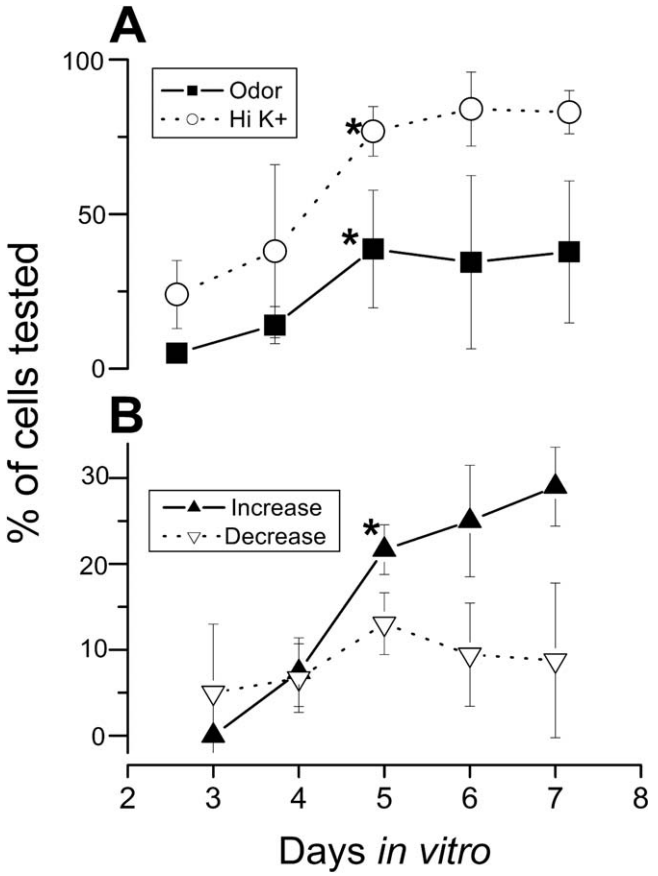

Fig. 4. The ability of all the PB cells to respond to odorants with increases or decreases in $[Ca^{2+}]_i$ changes over time. The data are from 14 individual runs. Cells were not tested on days 1 or 2 because of the low numbers of PB cells. Asterisks indicate the point at which responses attained a "steady state" (Welsch step-up procedure; for details see Materials and Methods). **A:** Cells responded to odors and K^+ depolarization by day 3; after day 5, their response rates do not increase appreciably over time. **B:** Details of the odor responses (solid squares) in A; note that the y-axis is different for this graph. At the first appearance of odor sensitivity, cells responded to odorants with either increases or decreases in $[Ca^{2+}]_i$ with equal frequency. As time progressed, the frequency of odorant-elicited increases and decreases in $[Ca^{2+}]_i$ both increase. Odorant-elicited $[Ca^{2+}]_i$ decreases and increases attained a steady state at day 4 and day 5, respectively.

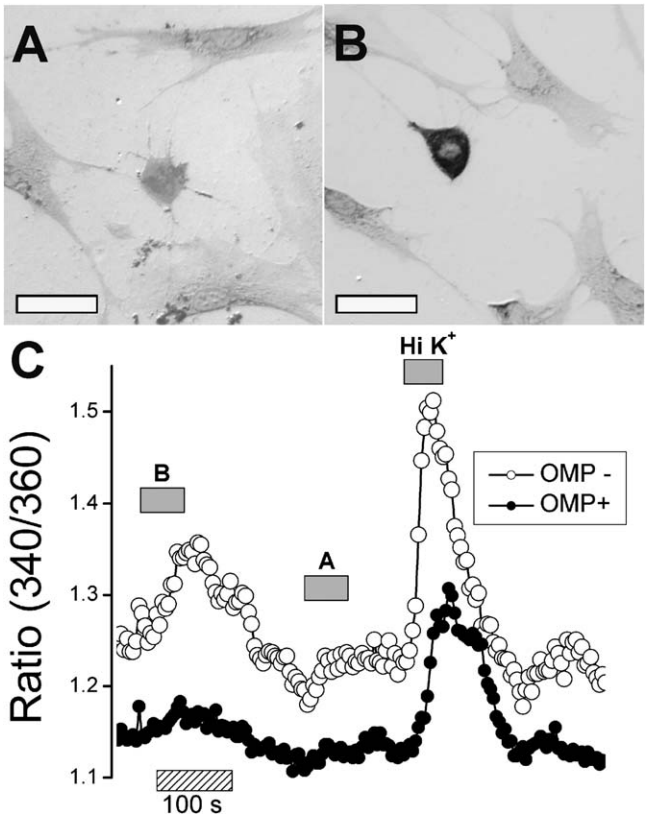

Fig. 5. Sample data from two different cells with different OMP immunoreactivity (**A:** OMP^-; **B:** OMP^+) from the same well of a six-well plate at day 6 and their responses to odorant stimulation (C). A: This cell that was OMP^- responded to mix B and to high K^+ with increases in $[Ca^{2+}]_i$ (Fig. 4C, open circles). **B:** A different cell from the same well that was OMP^+ did not respond to odor stimulation but responded to high K^+ with increases in $[Ca^{2+}]_i$ (Fig. 4C, solid circles). In **C**, stimulus applications (denoted by the solid bar) were 30–60 sec long; the time courses of the $[Ca^{2+}]_i$ changes are typical for these cells (Gomez et al., 2000). Time scale bar = 100 sec.

Depolarization-elicited $[Ca^{2+}]_i$ changes. Previous studies have shown that most rat ORNs responded to stimulation with a depolarizing concentration (135 mM) of K^+ (high K^+) with an increase in $[Ca^{2+}]_i$ (Restrepo et al., 1993a), indicating the neuronal identity by the presence of voltage-gated calcium channels. Interestingly, acutely isolated human ORNs rarely respond to high-K^+ stimulation (Rawson et al., 1997) with changes in $[Ca^{2+}]_i$. Our study used high K^+ to determine the possible state of neuronal differentiation of our hOEs. Figure 4A shows the proportion of high-K^+-responsive cells over time. Although the proportion of PD cells that responded to K^+ with a change in $[Ca^{2+}]_i$ did not change significantly over time, there is a significant increase in this K^+-responsive proportion of cells at day 5. Collectively, the results from Figure 4 suggest that functional maturity is likely attained within 4 days in vitro but that it takes 5 days to for the functional properties of entire population of hOEs to attain a steady state.

Correlation of Structural and Functional Maturation

Figure 5 shows a representative example of two different cells at day 6 from the same well of a six-well plate that showed different OMP immunoreactivity (OMP-, Fig. 5A; OMP^+, Fig 5B). Odor responses of these cells were measured by applying stimulus solutions one at a time (each application was followed by a wash with Ringer's solution) as described in Materials and Methods; the cells were subsequently immunostained for OMP and localized as described for Figure 1. The cells' responses to a stimulus application were clearly visible as a rise in $[Ca^{2+}]_i$ above the baseline, followed by a return to the

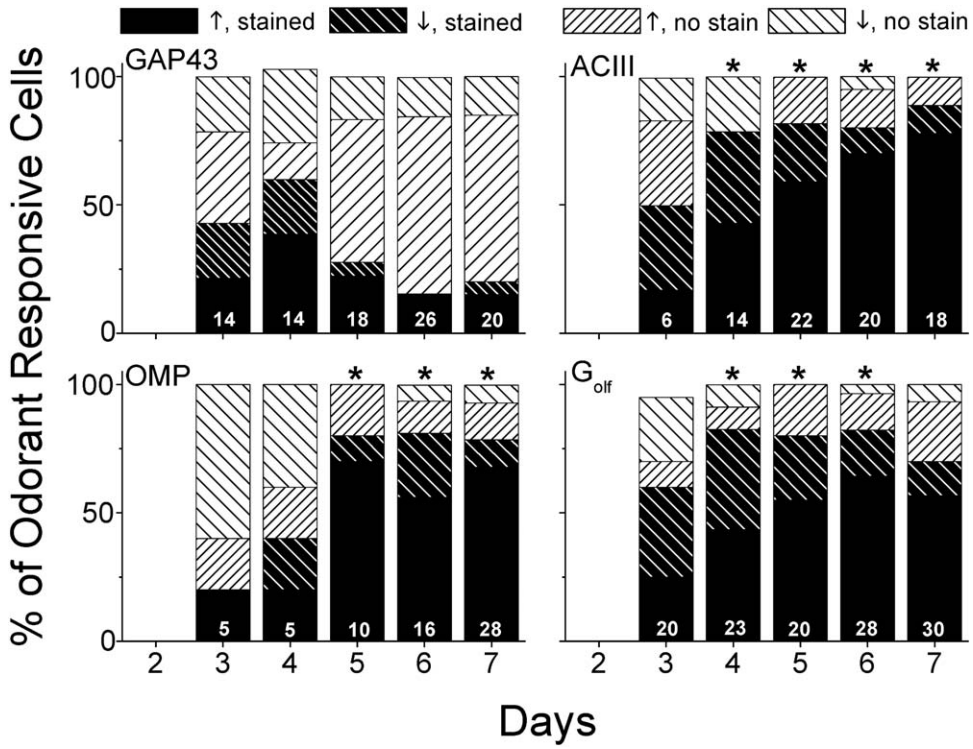

Fig. 6. Cells were passaged, and PB cells were tested as described for Figure 1 from days 3 through 7. The response type of each odorant-sensitive PB cell was determined (either increase [↑] or decrease [↓] in $[Ca^{2+}]_i$), and then tested for the presence of GAP43, G_{olf}, ACIII, or OMP as described in Figure 1. Only data from the PB cells are shown, because none of the PD cells expressed OMP. The number of cells that were counted for each day is shown in each bar. Asterisks show a statistically significant correlation between odorant sensitivity (either an increase or a decrease in $[Ca^{2+}]_i$ and molecular marker expression; kappa, $P < 0.05$). There was no correlation between odorant sensitivity and GAP43 expression at any point in time, but positive correlations between odorant sensitivity and ACIII, OMP, or G_{olf} emerged at days 4–5. There was no correlation between type of $[Ca^{2+}]_i$ response and molecular marker expression. It is interesting to note that none of the markers had a 100% correlation with odorant sensitivity, suggesting that odorant sensitivity is not completely dependent on the molecules traditionally associated with structural maturation.

baseline following stimulus removal. The OMP^- cell (Fig. 5A) responded to the odorant mix B, but not mix A, and to depolarization with high K^+, suggesting that OMP was not necessary for odorant sensitivity. In contrast, the OMP^+ cell (Fig. 5B) did not respond to either odorant mix; it was possible, however, that this cell was sensitive to other odorants that we did not test in the study.

Figure 6 shows a compilation of the results of the immunocytochemical staining and the odorant-elicited $[Ca^{2+}]_i$ responses as described in Figures 1 and 5. For this portion of the study, we focused only on the PB hOEs, because these were the cells that typically expressed OMP, a characteristic marker molecule of olfactory neurons. As in Figure 3, we also focused on four molecular markers, GAP43, OMP, ACIII, and G_{olf}. Because we counted data only from cells that we could unmistakably identify from the phase-contrast photograph taken at the end of the calcium imaging run, data from individual trials were sometimes sparse (one or two cells per well). Thus, data presented here were summed from all our individual trials.

We found no statistical correlation between odorant sensitivity and GAP43 expression across all days, suggesting that GAP43 was unrelated to the development of odorant sensitivity. During days 3 and 4, there were significant numbers of odorant-responsive hOEs that did not express OMP. Expectedly, this proportion shifted drastically on day 5, when OMP expression and odorant-sensitivity were tightly correlated (kappa, $P < 0.05$). At day 3 for both ACIII and G_{olf}, the proportion of odorant-sensitive cells that did not express these markers was sizeable. At day 4, the expression of these markers was correlated with odorant sensitivity; however, this proportion never reached 100%.

We attempted to determine whether there was a correlation between odorant response type (increase or decrease in $[Ca^{2+}]_i$; Fig. 4B) and molecular marker expression of hOEs. Because of the low numbers of cells, we could not do this for days 2 and 3. From days 4 through 6, we did not find any statistical correlation between response type and molecular marker expression.

DISCUSSION

The results of our study narrowed in on a time window in which cultured hOEs attain maturity. Previous studies

have shown that hOEs in vitro develop from precursors into odorant-responsive neurons that express key proteins such as odorant receptors (Borgmann-Winter et al., 2009). However, the results of our study suggest that odorant sensitivity per se do not indicate that cells have attained a "fully mature" state: a number of cells in our study were odorant sensitive prior to expressing molecules typical of mature ORNs in vivo.

In cultures derived from olfactory epithelial samples, there typically exists a mixed population of cells: most appear to be cells such as neuroblasts, olfactory ensheathing cells, or other glial cell types (Féron et al., 1998; Gomez et al., 2000; Liu et al., 2010). Previous studies on odorant sensitivity tested only cultured cells that were morphologically consistent (PB cells) with cultured hOEs from other species (Roskams et al., 1998; Gomez et al., 2000). The current study also looks at odorant sensitivity in the PD cells, which are generally regarded to be non-neuronal (Zhang et al., 2004; Liu et al., 2010). Some of the PD cells were clearly neuronal (NST^+), but it is unlikely that all of them were immature olfactory neurons; otherwise, the number of OMP^+ cells would have been very high by day 7 (OMP^+ cells at day 7 typically made up 5% or less of the overall cell population; personal observations).

From our results, we generated a hypothetical timeline of maturation of hOEs in vitro. At day 2, the culture consisted almost exclusively of PD cells, some of which were likely precursors or immature neurons in different stages of maturation that are $NCAM^+$, NST^+, and $GAP43^+$ (Ensoli et al., 1998). Previous studies have shown that, under these culture conditions, many of these PD cells express markers for glial cells such as GFAP, S100β, TrkA, nestin, CK5, and peripherin (Gomez et al., 2000; Roisen et al., 2001; Zhang et al., 2004, 2006; Borgmann-Winter et al., 2009).

At day 3, PB hOEs were visible, and a subset of the cells in culture began to express proteins necessary for mediating odorant sensitivity: although they were still $GAP43^+$, some coexpressed ACIII and G_{olf}, were odorant-sensitive, and expressed voltage-gated calcium channels (and were thus sensitive to high K^+). A small proportion of PB hOEs that were visible in culture was OMP-negative (Fig. 5) but odorant sensitive (Fig. 4). Once these cells began to express OMP, GAP43 expression was terminated. Interestingly, some PD cells also expressed ACIII or G_{olf}, suggesting that these were differentiating neurons. It is at this stage that mechanisms for odorant-elicited decreases are expressed (see below).

At day 4, a small proportion of PB hOEs began to express OMP. A larger proportion of PB hOEs was $ACIII^+$ or $G_{olf}{}^+$ and odorant-sensitive, suggesting that the mechanisms for odorant sensitivity develop prior to the expression of proteins that are likely involved with structural attributes of olfactory neurons. At day 5, the number of "functionally mature" PB hOEs reaches a steady state: expression of ACIII or G_{olf} (Fig. 3), odorant sensitivity rates (Fig. 4), or proportion of cells that respond to high K^+ (Fig. 4) did not significantly increase after day 5. In addition, more precursors and immature PB neurons at later stages in development continued to propagate in culture: a sizable portion of cells are sensitive to Hi K^+, and a small proportion of $GAP43^+$ cells is seen at these later stages. At day 6, OMP expression in PB hOEs attained a steady state (Fig. 3) and was significantly correlated with odorant sensitivity (Fig. 5). It was therefore assumed that the entire maturation process of hOEs was complete at this point. Because the culture was mixed, the surviving precursors likely continued to generate new immature neurons, thus accounting for the small proportion of odorant-sensitive, OMP-negative PB cells.

Under the conditions of our experiment, OMP did not appear to be necessary for functional development. Studies have suggested the necessity of OMP for development of odor-mediated behaviors (Lee et al., 2011), but other studies with OMP knockout mice have shown an alteration but not a complete loss of olfactory neuron responses (Buiakova et al., 1996; Youngentob and Margolis, 1999; Reisert et al., 2007) or showed compromised cellular mechanisms associated with odor-induced calcium fluxes (Kwon et al., 2009). Our study did not test features (such as threshold, time course, or pharmacological sensitivity) of the odorant-elicited $[Ca^{2+}]_i$ responses. Thus it is possible that, although OMP plays an important role in maturation of olfactory neurons in vivo, the pathways controlled by OMP may not be fully operational or developmentally related in vitro.

Interestingly, the mechanisms for odorant sensitivity most likely develop earlier than do the structural proteins. Evidence from rodents suggests that ORN maturation occurs as the neurons target their appropriate glomeruli in the olfactory bulb (Schwob et al., 1992; Schwob, 2002) and that the olfactory bulb provides trophic support for the neurons. As the ORNs develop in vivo, immature neurons are odorant sensitive prior to their axons reaching their final targets in the olfactory bulb; developing ORNs express molecules such as olfactory receptor proteins that assist them in targeting the appropriate glomeruli during development. Our in vitro results support the notion that the development of odorant sensitivity occurs early in the maturation process.

We note a number of other curious results from these experiments. First, a some hOEs that were odorant-sensitive were also $ACIII^-$ or $G_{olf}{}^-$; this proportion was close to 50% at day 3 and 20–30% on the succeeding days. The widely accepted model of odor signal transduction in vertebrates suggests that odorants bind to receptors that activate signal transduction pathways that produce cAMP (for review see Schild and Restrepo, 1998), thus necessitating the involvement of both G_{olf} and ACIII. In contrast, other studies suggest the human olfactory system may also utilize alternate signal transduction pathways that do not involve cAMP (in acutely isolated ORNs: Restrepo et al., 1993b; Rawson et al., 1997; in olfactory cultures: Gomez et al., 2000). It is therefore possible that the $G_{olf}{}^-/ACIII^-$ odorant-sensitive cells utilize such alternate pathways for odor signaling. However, we cannot discount the notion that the developmental process in

vitro results in the emergence of alternate previously undescribed phenotypes that are not normally present in vivo; this possibility remains to be tested.

Another curious result was the preponderance of odorant-elicited decreases in $[Ca^{2+}]_i$ early in the developmental timeline. In hOEs in vitro, the proportion of odorant-elicited increases vs. decreases is typically 3:1 (Gomez et al., 2000). In this study, the frequency of odorant-elicited decreases in $[Ca^{2+}]_i$ at days 2 and 3 was about the same as that of odorant-elicited increases in $[Ca^{2+}]_i$. Although it is generally accepted that odorant-elicited $[Ca^{2+}]_i$ increases are mediated by an influx of Ca^{2+} through the second-messenger-gated channels and through voltage-gated Ca^{2+} channels (for review see Schild and Restrepo, 1998), the mechanism for eliciting an odorant-elicited decrease in $[Ca^{2+}]_i$ is still unknown. There is strong evidence for the involvement of Na^+/Ca^{2+} exchangers in olfactory neurons (Noe et al., 1997; Lucero et al., 2000), which likely mediate Ca^{2+} extrusion and the subsequent cellular adaptation following stimulation (Jung et al., 1994; Reisert and Matthews, 1998, 2001). Because the mechanisms for driving increases or decreases in $[Ca^{2+}]_i$ are very different, it is possible that these mechanisms develop separately and that the mechanism for expression of cellular components for calcium removal from the cytosol is functional prior to the development of second messenger systems (the voltage-gated channels are developed and functional by day 3, as shown in Fig. 4A).

Previously, studies have focused on the structure and function of the PB hOEs as the in vitro representatives of in vivo ORN function. These PB hOEs are capable of expressing a diversity of receptor proteins (olfactory, dopamine, and N-methyl-D-aspartate receptors; Borgmann-Winter et al., 2009), demonstrating their similarity to ORNs in vivo. The PD cells were thought to be the primary cells that drive and guide neuronal development (Ensoli et al., 1998; Roisen et al., 2001; Higginson and Barnett, 2011) and have been used for studies on spinal cord regeneration because of their endogenous secretion of neurotrophic factors (Garcia-Alias et al., 2004). Our study suggests the important role of the PD cells in olfactory neurogenesis and an important avenue for future investigation: these cells may be expressing a number of key proteins involved in the development of olfactory function, either as immature neurons or as cells that promote olfactory neurogenesis.

ACKNOWLEDGMENTS

We are deeply indebted to Dr. Nancy Rawson for providing the cells used in the project. This work was part of the undergraduate Honors Thesis research of S.A.Y. We also thank Ms. Jennifer Crockett Ho for her assistance in conducting the experiments.

REFERENCES

Armitage P, Colton T. 1998. Encyclopedia of biostatistics. New York: John Wiley & Sons. 4898 p.

Bakalyar HA, Reed RR. 1990. Identification of a specialized adenylyl cyclase that may mediate odorant detection. Science 250:1403–1406.

Borgmann-Winter KE, Rawson NE, Wang H-Y, Wange H, MacDonald ML, Ozdener MH, Yee KK, Gomez G, Xu J, Bryant B, Adamek GMirzai N, Pribitkin E, Hahn C-G. 2009. Human olfactory epithelial cells generated in vitro express diverse neuronal characteristics. Neuroscience 158:642–653.

Buiakova OI, Baker H, Scott JW, Farbman A, Kream R, Grillo M, Franzen L, Richman M, Davis LM, Abbondanzo S, Stewart CL, Margolis FL. 1996. Olfactory marker protein (OMP) gene deletion causes altered physiological activity of olfactory sensory neurons. Proc Natl Acad Sci U S A 93:9858–9863.

Calof AL, Hagiwara N, Holcomb JD, Mumm JS, Shou J. 1996. Neurogenesis and cell death in olfactory epithelium. J Neurobiol 30:67–81.

Calof AL, Mumm JS, Rim PC, Shou J. 1998. The neuronal stem cell of the olfactory epithelium. J Neurobiol 36:190–205.

Ensoli F, Fiorelli V, Vannelli GB, Barni T, De Cristofaro M, Ensoli B, Thiele CJ. 1998. Basic fibroblast growth factor supports human olfactory neurogenesis by autocrine/paracrine mechanisms. Neuroscience 86:881–893.

Féron F, Perry C, McGrath J, Mackay-Sim A. 1998. New techniques for biopsy and culture of human olfactory epithelial neurons. Arch Otolaryngol Head Neck Surg 124:861–866.

Garcia-Alias G, Lopez-Vales R, Fores J, Navarro X, Verdu E. 2004. Acute transplantation of olfactory ensheathing cells or Schwann cells promotes recovery after spinal cord injury in the rat. J Neurosci Res 75:632–641.

Gomez G, Rawson NE, Hahn C-G, Micahels R, Restrepo D. 2000. Characteristics of odorant elicited calcium changes in cultured human olfactory neurons. J Neurosci Res 62:737–749.

Higginson JR, Barnett SC. 2011. The culture of olfactory ensheathing cells (OECs)—a distinct glial cell type. Exp Neurol 229:2–9.

Jung A, Lischka FW, Engel J, Schild D. 1994. Sodium/calcium exchanger in olfactory receptor neurones of *Xenopus laevis*. Neuroreport 5:1741–1744.

Kwon HJ, Koo JH, Zufall F, Leinders-Zufall T, Margolis FL. 2009. Ca^{2+} extrusion by NCX is compromised in olfactory sensory neurons of $OMP^{-/-}$ mice. PLOS ONE 4:e4260.

Lee AC, He J, Ma M. 2011. Olfactory marker protein is critical for functional maturation of olfactory sensory neurons and development of mother preference. J Neurosci 23:2974–2982.

Liu K, Li Y, Wang H, Jiang X, Zhao Y, Sun D, Chen L, Young W, Huang H, Zhou C. 2010. The immunohistochemical characterization of human fetal olfactory bulb and olfactory ensheathing cells in culture as a source for clinical CNS restoration. Anat Rec 293:359–369.

Lowry LD, Pribitkin EA. 1995. Collection of human olfactory tissue. In: Spielman AI, Brand JG, editors. Experimental biology of taste and olfaction. Boca Raton, FL: CRC Press. p 47–48.

Lucero MT, Huang W, Dang T. 2000. Immunohistochemical evidence for the Na^+/Ca^{2+} exchanges in squid olfactory neurons. Phil Trans Roy Soc Lond B 355:1215–1218.

Mackay-Sim A. 2012. Patient-derived olfactory stem cells: new models for brain diseases. Stem Cell 30:2361–2365.

Margolis F. 1980. A marker protein for the olfactory chemoreceptor neuron. In: Barshaw RA, Schneider DM, editors. Proteins of the nervous system. New York: Raven Press. pp 59–84.

Matigian N, Abrahamsen G, Sutharsan R, Cook AL, Vitale AM, Nouwens A, Bellette B, An J, Anderson M, Beckhouse AG, Bennebroek M, Cecil R, Chalk AM, Cochrane J, Fan Y, Feron F, McCurdy R, McGrath JJ, Murrell W, Perry C, Raju J, Ravishankar S, Silburn PA, Sutherland GT, Mahler S, Mellick GD, Wood SA, Sue CM, Wells CA, Mackay-Sim A. 2010. Disease-specific, neurosphere-derived cells as models for brain disorders. Dis Model Mech 3:785–798.

Morrison, EE, Costanzo RM. 1992. Morphology of olfactory epithelium in humans and other vertebrates. Mircosc Res Techniq 23:49–61.

Murdoch B, Roskams AJ. 2007. Olfactory epithelium progenitors: insights from transgenic mice and in vitro biology. J Mol Hist 38:581–599.

Murrell W, Bushell GR, Livesey J, McGrath J, MacDonald KPA, Bates PR, Mackay-Sim A. 1996. Neurogenesis in adult human. Neuroreport 7:1189–1194.

Noe J, Tarelius E, Boekhoff I, Breer H. 1997. Sodium/calcium exchanger in rat olfactory neurons. Neurochem Int 30:523–531.

Ozdener MH, Rawson NE. 2004. Olfactory dysfunction in neurodegenerative diseases. Eur J Gen Med 1:1–11.

Rawson NE, Gomez G. 2002. Cell and molecular biology of human olfaction. Microsc Res Techniq 58:142–151.

Rawson NE, Gomez G, Coward B, Brand JG, Lowry LD, Pribitkin EA, Restrepo D. 1997. Selectivity and response characteristics of human olfactory neurons. J Neurophysiol 77:1606–1613.

Reed R. 1992. Signaling pathways in odorant detection. Neuron 8:205–209.

Reisert J, Matthews HR. 1998. Na^+-dependent Ca^{2+} extrusion governs response recovery in frog olfactory receptor neurons. J Gen Physiol 112: 529–535.

Reisert J, Matthews HR. 2001. Response properties of isolated mouse olfactory receptor cells. J Physiol 530:113–122.

Reisert J, Yau K-W, Margolis FL. 2007. Olfactory marker protein modulates the cAMP kinetics of the odour-induced response in cilia of mouse olfactory receptor neurons. J Gen Physiol 585:731–740.

Restrepo D, Okada Y, Teeter JH. 1993a. Odorant-regulated Ca^{2+} gradients in rat olfactory neurons. J Gen Physiol 102:907–924.

Restrepo D, Okada Y, Teeter JH, Lowry LD, Cowart B. 1993b. Human olfactory neurons respond to odor stimuli with an increase in cytoplasmic Ca^{2+}. Biophys J 64:1961–1966.

Roisen FJ, Klueber KM, Lu CL, Hatcher LM, Dozier A, Shields CB, Maguire S. 2001. Adult human olfactory stem cells. Brain Res 890:11–22.

Roskams AJI, Cai X, Ronnet GV. 1998. Expression of neuron-specific beta-III tubulin during olfactory neurogenesis in the embryonic and adult rat. Neuroscience 83:191–200.

Schild D, Restrepo D. 1998. Transduction mechanisms in vertebrate olfactory receptor cells. Physiol Rev 78:429–466.

Schwob JE. 2002. Neural regeneration and the peripheral olfactory system. Anat Rec 269:33–49.

Schwob JE, Szumowski KE, Stasky AA. 1992. Olfactory sensory neurons are trophically dependent on the olfactory bulb for their prolonged survival. J Neurosci 12:3896–3919.

Sokal RR, Rohlf FJ. 1994. Biometry: the principles and practices of statistics in biological research, 3rd ed. New York: W.H. Freeman. 880 p.

Vannelli GB, Ensoli F, Zonefrati R, Kubota Y, Arcangeli A, Becchetti A, Camici G, Barni T, Thiele CJ, Balboni GC. 1995. Neuroblast long-term cell cultures from human fetal olfactory epithelium respond to odors. J Neurosci 15:5382–4394.

Vawter MP, Basaric-Keys J, Li Y, Lester DS, Lebovics RS, Lesch KP, Kulaga H, Freed WJ, Sunderland T, Wolozin B. 1996. Human olfactory neuroepithelial cells: tyrosine phosphorylation and process extension are increased by the combination of IL-1β, IL-6, NGF, and bFGF. Exp Neurobiol 142:179–194.

Wolozin B, Sunderland T, Zheng B, Resau J, Dufy B, Barker J, Swerdlow R, Coon H. 1992. Continuous culture of neuronal cells from adult human olfactory epithelium. J Mol Neurosci 3:137–146.

Youngentob SL, Margolis FL. 1999. OMP gene deletion causes and elevation in behavioral threshold sensitivity. Neuroreport 10:15–19.

Zhang X, Klueber KM, Guo Z, Lu C, Roisen FJ. 2004. Adult human olfactory neural progenitors cultured in defined medium. Exp Neurol 186:112–123.

Zhang X, Klueber KM, Guo Z, Cai J, Lu C, Winstead WI, Qiu M, Roisen FJ. 2006. Induction of neuronal differentiation of adult human olfactory neuroepithelial-derived progenitors. Brain Res 1073–1074: 109–119.